deficient mdx myofibers still improved the mdx phenotype.
日本遺伝子治療学会, 東京, 8.5, 2004

14. Yuasa K, Yoshimura M, Urasawa N, Sato K, Miyagoe-Suzuki Y, Howell MJ, Takeda S:
Successful AAV vector-mediated gene transfer into canine skeletal muscle required suppression of excess immune responses.
日本遺伝子治療学会, 東京, 8.5, 2004
15. 上住聡芳, 尾嶋孝一, 増田智, 深瀬明子, 鈴木友子, 武田伸一:
骨格筋再生過程における side population (SP) cells の解析。
第 25 回日本炎症・再生医学会, 東京, 7.14, 2004
16. 望月靖史, 尾嶋孝一, 上住聡芳, 増田智, 武田伸一:
骨格筋の脱神経病変に対する骨髄由来細胞の関与
第 25 回日本炎症・再生医学会, 東京, 7.13, 2004
17. 武田伸一:
筋ジストロフィーモデル動物における遺伝子治療研究の現況と展望。
三菱ウエルファーマ 横浜 5.28, 2004
18. 武田伸一:
筋ジストロフィーモデル動物における遺伝子治療研究の現況と展望。
第 45 回日本神経学会総会シンポジウム 東京 5.14, 2004
19. 吉村まどか, 池本 円, 坂本美喜, 望月靖史, 湯浅勝敏, 辻 省次, 武田伸一:
アデノ随伴ウイルス (AAV) ベクターによるマイクロ・ジストロフィン遺伝子の導入効果
第 45 回日本神経学会総会, 東京, 5.14, 2004
20. 上住聡芳, 尾嶋孝一, 深田宗一朗, 増田 智, 深瀬明子, 鈴木友子, 武田伸一:
骨格筋再生過程による Side Population (SP) 細胞の解析
第 2 回幹細胞シンポジウム, 4.26, 2004.

H. 知的所有権の出願・登録状況

なし

研究成果の刊行に関する一覧表

雑誌

発表者氏名	論文タイトル名	発表誌名，巻号：ページ，出版年
Takahashi J, Itoh Y, Fujimori K, Imamura M, Wakayama Y, Miyagoe-Suzuki Y, Takeda S:	The utrophin promoter A drives high expression of the transgenic LacZ gene in liver, testis, colon, submandibular gland, and small intestine.	*J Gene Medicine*, **7**(2): 237-48, 2004
Yoshimura M, Sakamoto M, Ikemoto M, Mochizuki Y, Yuasa K, Miyagoe-Suzuki Y, Takeda S:	AAV vector-mediated micro-dystrophin expression in a relatively small percentage of mdx myofibers improved the mdx phenotype.	*Mol Ther*, **10**(5): 821-8, 2004
Ojima K, Uezumi A, Miyoshi H, Masuda S, Morita Y, Fukase A, Hattori A, Nakauchi H, Miyagoe-Suzuki Y, Takeda S:	Mac-1^{low} early myeloid cells in the bone marrow-derived SP fraction migrate into injured skeletal muscle and participate in muscle regeneration.	*Biochem Biophys Res Commu*, 2004 Sep 3; **321**(4): 1050-61
Gawlik K, Miyagoe-Suzuki Y, Ekblom P, Takeda S, Durbeej M:	Laminin alpha 1 chain reduces muscular dystrophy in laminin alpha 2 chain deficient mice.	*Hum Mol Genet*, 2004, **13**(16): 1775-84.
Fukada S, Higuchi S, Segawa M, Koda K, Yamamoto Y, Tsujikawa K, Kohama Y, Uezumi A, Imamura M, Miyagoe-Suzuki Y, Takeda S, Yamamoto H:	Purification and cell-surface marker characterization of quiescent satellite cells from murine skeletal muscle by a novel monoclonal antibody.	*Exp Cell Res*, 2004 Jun 10; **296**(2): 245-55.
Nishiyama A, Endo T, Takeda S, Imamura M:	Identification and characterization of ε-sarcoglycans in the central nervous system.	*Mol Brain Res*, **125**(1-2): 1-12, 2004
Munehira Y, Ohnishi T, Kawamoto S, Furuya A, Shitara K, Imamura M, Yokota T, Takeda S, Amachi T, Matsuo M, Kioka N, Ueda K:	alpha 1-syntrophin modulates turnover of ABCA1.	*J Biol Chem*, **279**(15): 15091-5, 2004
Kino Y, Oma Y, Sasagawa N, Ishiura S:	Muscleblind protein, MBNL1/EXP, binds specifically to CHHG repeats.	*Hum Mol Genet*, **13**: 495-507, 2004
Watanabe T., Takagi, A., Sasagawa N, Ishiura S, Nakase H:	Altered expression of CUG binding protein 1 mRNA in myotonic dystrophy 1: possible RNA-RNA interaction.	*Neurosci Res*, **49**: 47-54, 2004

THE JOURNAL OF GENE MEDICINE
J Gene Med 2005; 7: 237–248.
Published online 10 November 2004 in Wiley InterScience (www.interscience.wiley.com). DOI: 10.1002/jgm.651

RESEARCH ARTICLE

The utrophin promoter A drives high expression of the transgenic *LacZ* gene in liver, testis, colon, submandibular gland, and small intestine

Joji Takahashi[1,2]
Yuka Itoh[1]
Keita Fujimori[3]
Michihiro Imamura[1]
Yoshihiro Wakayama[2]
Yuko Miyagoe-Suzuki[1]
Shin'ichi Takeda[1]*

[1]*Department of Molecular Therapy, National Institute of Neuroscience, National Center of Neurology and Psychiatry, 4-1-1 Ogawa-higashi, Kodaira, Tokyo 187-8502, Japan*

[2]*Department of Neurology, Showa University Fujigaoka Hospital, 1-30 Fujigaoka, Aoba-ku, Yokohama 227-8501, Japan*

[3]*Department of Ophthalmology, Akita University School of Medicine, 1-1-1 Hondo, Akita 010-8543, Japan*

*Correspondence to:
Shin'ichi Takeda, Department of Molecular Therapy, National Institute of Neuroscience, National Center of Neurology and Psychiatry, 4-1-1 Ogawa-higashi, Kodaira, Tokyo 187-8502, Japan. E-mail: takeda@ncnp.go.jp

Received: 30 March 2004
Revised: 31 May 2004
Accepted: 1 June 2004

Abstract

Background Duchenne muscular dystrophy (DMD) is caused by the absence of the muscle cytoskeletal protein dystrophin. Utrophin is an autosomal homologue of dystrophin, and overexpression of the protein is expected to compensate for the defect of dystrophin. The *utrophin* gene has two promoters, A and B, and promoter A of the *utrophin* gene is a possible target of pharmacological interventions for DMD because A-utrophin is up-regulated in dystrophin-deficient *mdx* skeletal and cardiac muscles. To investigate the utrophin promoter A activity *in vivo*, we generated nuclear localization signal-tagged *LacZ* transgenic mice, where the *LacZ* gene was driven by the 5-kb flanking region of the A-*utrophin* gene.

Methods Four transgenic lines were established by mating four independent founders with C57BL/6J mice. The levels of mRNA for β-galactosidase in several tissues were examined by RT-PCR. Cryosections from several tissues were stained with hematoxylin and eosin (H&E) and with 5-bromo-4-chloro-3-indolyl-β-D-galactopyranoside (X-Gal).

Results The 5-kb upstream region of the A-*utrophin* gene showed high transcriptional activity in liver, testis, colon, submandibular gland, and small intestine, consistent with the endogenous expression of utrophin protein. Surprisingly, the levels of both β-gal protein and mRNA for the transgene in cardiac and skeletal muscles were extremely low, even in nuclei near the neuromuscular junctions. These results indicate that the regulation of the *utrophin* gene in striated muscle is different from that in non-muscle tissues.

Conclusions Our results clearly showed that the utrophin A promoter is not sufficient to drive expression in muscle, but other regulatory elements are required.

Keywords Duchenne muscular dystrophy; dystrophin; utrophin; promoter; β-galactosidase

Introduction

Duchenne muscular dystrophy (DMD) is an X-linked lethal disorder caused by a defect in the *DMD* gene, which encodes a large cytoskeletal protein, dystrophin [1]. Dystrophin is normally expressed on the subsarcolemma and interacts with dystrophin-associated-proteins (DAPs) [2–5]. These proteins link the cytoskeleton of myofibers to the extracellular matrix and maintain the integrity of muscle fibers. The

lack of dystrophin in DMD prevents the assembly of DAPs on the sarcolemma and leads to massive muscle necrosis, resulting in cardiomyopathy and early death.

Utrophin is a 395-kDa cytoskeletal protein with a high degree of amino acid identity with dystrophin [6,7]. It is ubiquitously expressed in most tissues. In embryonic and neonatal skeletal muscles, it is expressed both synaptically and extra-synaptically. In adult skeletal muscle, it is found only at the postsynaptic membrane of the neuromuscular junction (NMJ) and the myotendinous junction [8,9]. During muscle regeneration, it transiently reappears at the sarcolemma of immature muscle fibers [10].

Previous transgenic experiments showed that overexpression of utrophin at the sarcolemma compensates for the lack of dystrophin function and ameliorates dystrophic phenotypes in dystrophin-deficient *mdx* mice [11–13]. Similarly, it has been shown that adenovirally induced utrophin improves dystrophic changes in *mdx* mice [14]. We previously reported that adenovirally transferred β-galactosidase (β-gal) expression evoked up-regulation of endogenous utrophin, resulting in partial amelioration of dystrophic phenotypes of dystrophin-deficient *mdx* muscle [15]. These findings suggest that up-regulation of endogenous utrophin is an alternative strategy for DMD therapy.

Transcriptional regulation of the *utrophin* gene is more complicated than previously pictured. There are two full-length utrophin mRNAs, A and B, with different N termini, which are driven by two distinct promoters [16,17]. Further, it has been shown that transcription of A-utrophin is augmented by an intronic enhancer [18]. Both A- and B-utrophin mRNA are expressed in a tissue-specific manner, and an immunohistochemical study showed that A-utrophin is expressed at the NMJ, choroid plexus, pia mater, and renal glomerulus and tubule, and is up-regulated in regenerating muscle and in *mdx* muscle [19,20]. On the other hand, B-utrophin is expressed in vascular endothelial cells [20]. Several short utrophin isoforms have also been reported, as found in dystrophin [21]. Importantly, there is some evidence suggesting that the expression of utrophin is regulated at multiple levels, including transcription, targeting of transcripts and regulation of mRNA stability. In particular, the stability of transcripts is regulated mainly by the interaction of the 3′-untranslated region (3′-UTR) of utrophin mRNA with sequence-specific RNA binding proteins [22,23].

We previously reported that local administration of recombinant interleukin-6 (rIL-6) elevated the level of utrophin at the sarcolemma in dystrophin-deficient *mdx* muscle, although the effects continued for only a short time [24]. To further elucidate the transcriptional regulation of utrophin in skeletal muscle, we generated transgenic mice in which the *LacZ* gene is driven by the 5320-bp 5′-flanking region containing the utrophin A core promoter. Here we show that the 5-kb upstream region of A-utrophin drives strong expression of nuclear localization signal (nls)-tagged β-gal expression in cells adjacent to basal lamina in liver, testis, colon, submandibular gland, and small intestine, but shows extremely low transcriptional activity in skeletal and cardiac muscles.

Materials and methods

Construction of the transgene and generation of transgenic mice

Genomic fragments containing the 5′ end of the mouse A-*utrophin* gene were cloned from a 129Sv mouse genomic library (Stratagene). One clone contained the 5320-bp 5′-flanking region of the A-*utrophin* gene, the complete exon 1A and the first 59 bp of the exon 2 UTR. The genomic fragment was fused in-frame to an nls (from SV40T antigen)-tagged *LacZ* gene [25] (pCMVb, Clontech) followed by a rabbit β-globin poly A signal in Bluescript II (Stratagene) (see also Figures 1A and 1B). The DNA fragment containing the transgene expression cassette was purified from an agarose gel and injected into C57BL/6J fertilized eggs by GenCom (Machida, Tokyo, Japan) (see also Figure 1C). We obtained four transgenic F_0 (utrophin promoter A/nls-LacZ transgenic (Tg)) mice, and four transgenic lines were established by mating founders with C57BL/6J mice (B6). To obtain transgenic *mdx* (Tg/*mdx*) male mice, transgene-positive F_1 males were mated with *mdx* females (also see Figure 1D).

Animals

B6 and *mdx* mice aged 8–10 weeks, Tg mice and their wild-type littermates aged 3–18 weeks, and Tg/*mdx* mice aged 2–4 weeks were used. All animals were housed in a separate room with controlled temperature (20–22 °C) and under an artificial lighting regime (12 h light/12 h dark). Tg mice were 5 weeks old and Tg/*mdx* mice were 2 weeks old when they were anesthetized by inhalation of diethyl ether (Wako Chemicals, Japan), and cardiotoxin or rIL-6 was injected into their tibialis anterior (TA) muscles. Animals were sacrificed by cervical dislocation. All protocols were approved by the Institutional Animal Care and Use Committee of the National Institute of Neuroscience and were performed in compliance with the "Guide for the Care and Use of Animals" of the Division of Laboratory Animal Resources.

Genotyping

Tg mice were screened by Southern blot analysis of genomic DNA from their tails. Genomic DNA was isolated using a lysis buffer (50 mM Tris-HCl, pH 8.0, 0.1 M NaCl, 20 mM EDTA, 1% SDS) with proteinase K (0.15 mg/ml) and pronase E (1 mg/ml) digestion. Genomic DNA (10 μg) was digested by *BamH* I, separated on a 0.8% agarose gel, and transferred onto Hybond-N^+ membranes (Amersham Biosciences, UK). A 3072-bp DNA fragment of the *LacZ* gene was labeled with ^{32}P-dCTP as a Southern

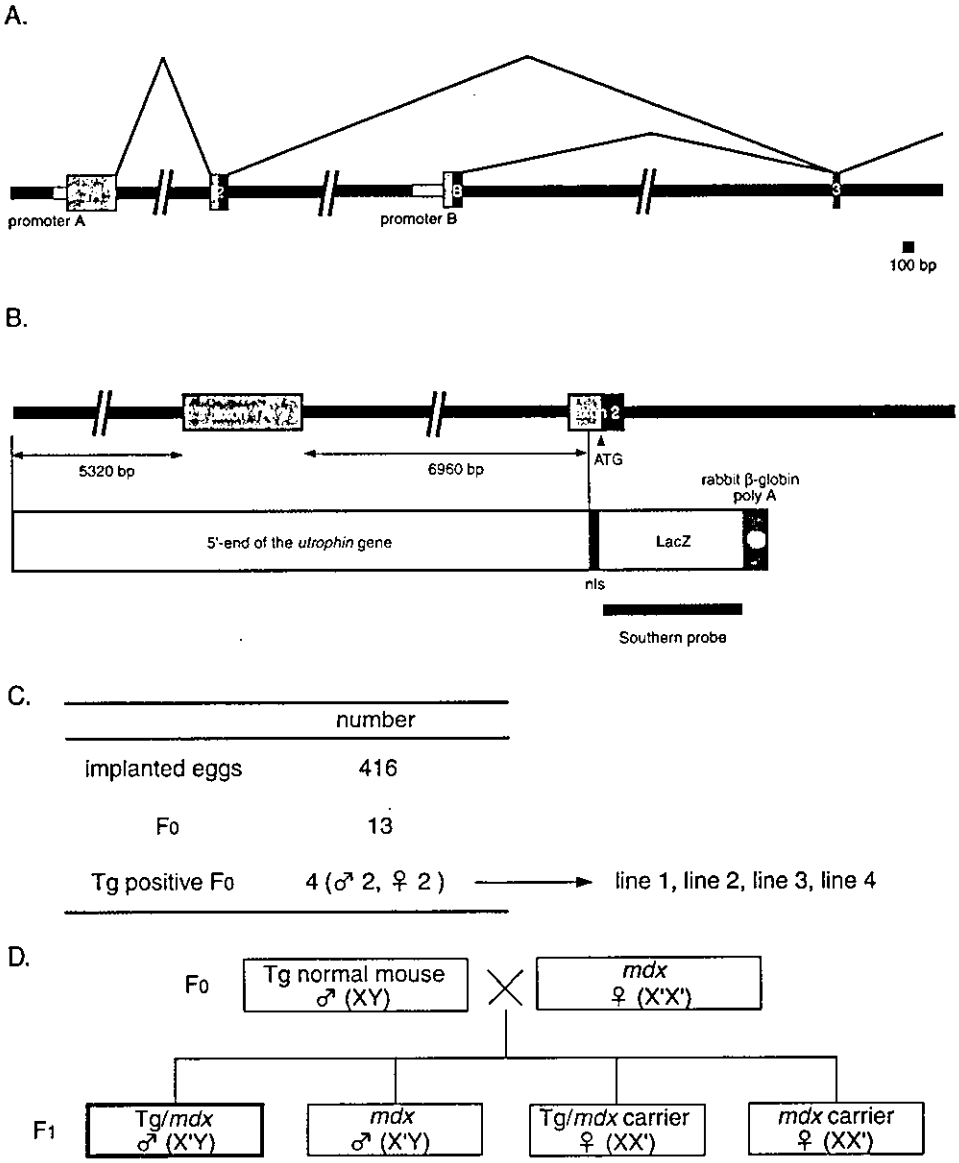

Figure 1. Generation of the A-utrophin promoter/nls LacZ transgenic mice. (A) Structure of the 5′ end of the *utrophin* gene. The *utrophin* gene is transcribed by two A and B promoters (white lines) that give rise to two transcripts, A-utrophin mRNA and B-utrophin mRNA, respectively. The two utrophin transcripts have different N-termini. Gray boxes indicate the 5′-UTR. Black boxes indicate the translated region of the exon. Scale bar indicates 100 bp. (B) Diagram of the transgene used in this study. The genomic fragment (12.4 kb), which contained the 5320-bp 5′-flanking region of the A-*utrophin* gene, exon 1A, and the first 59 bp of exon 2 UTR, was fused in-frame to a nls-tagged *LacZ* gene. Black bar indicates the Southern probe used to determine genotypes. (C) Summary of generation of transgenic mice. (D) Generation of transgenic *mdx* mice. Bold box indicates transgenic *mdx* male mice used in this study

probe, and hybridized with membranes at 65 °C overnight. The membranes were then washed extensively (2× SSPE, 0.1% SDS; 1× SSPE, 0.1% SDS; 0.1× SSPE, 0.1% SDS) at 65 °C and analyzed by BAS 2500 (Fuji Film, Japan).

Isolation of total RNA

Three-week-old Tg mice and wild-type littermates were sacrificed, and tissues were isolated and rapidly frozen in liquid nitrogen. Total RNA was isolated from frozen tissues using TRIzol reagent (Invitrogen Life Technologies, USA) according to the manufacturer's protocol. Finally, total RNA was treated with 1 U of RNase-free DNase I (Invitrogen Life Technologies) per microgram of RNA at room temperature for 15 min, and DNase I was inactivated by the addition of 25 mM EDTA (pH 8.0) and heating at 65 °C for 10 min.

Reverse transcription (RT)-PCR

RT was performed with 3.5 μg of total RNA using SuperScript II™ (Invitrogen Life Technologies) according to the manufacturer's protocol. PCR was performed using the *utrophin* exon 1A sense (5′-GGCGTTTCCAATCGGGTGTC-3′) and the *LacZ* gene antisense (5′-GCGGGCCTCTTCGCTATTAC-3′) primers for 35

cycles (denaturation at 95 °C for 1 min, annealing at 59 °C for 30 s, and extension at 72 °C for 1 min). As a control for the generation of PCR products due to residual contamination of genomic DNA, an equivalent amount of RNA that had not been treated with RT was also tested in parallel. The RT-PCR products of all samples were compared with the levels for a housekeeping gene, 18s rRNA, amplified with the following primer pair: sense primer (5′-TACCCTGGCGGTGGGATTAAC-3′) and anti-sense primer (5′-CGAGAGAAGACCACGCCAAC-3′). Amplification of A-utrophin was performed with the following primer pair: the *utrophin* gene exon 1A sense primer (5′-GGCGTTTCCAATCGGGTGTC-3′) and the *utrophin* gene exon 2 anti-sense primer (5′-CGTTCTGCCCATCATCAGGC-3′).

5′ RACE analysis

5′ RACE was carried out using the 5′ RACE system for rapid amplification of cDNA ENDs, V.2 kit (Invitrogen Life Technologies) following the manufacturer's protocol. Total RNA was reverse-transcribed using the *LacZ* gene-specific primer (GSP)-1 (5′-CGGATTGACCGTAATGGGATA-3′). The anchor-ligated cDNA was then PCR-amplified using the abridged anchor primer provided and the *LacZ* gene anti-sense primer, which was designed upstream of GSP-1, GSP-2 (5′-GCGGGCCTCTTCGCTATTAC-3′). In addition, the primary PCR product was amplified using the abridged universal amplification primer provided and the *nls* anti-sense primer, GSP-3 (5′-CGCTCATGATGCACGGTCTG-3′) designed upstream of GSP-2. PCR products were cloned into a pCR2.1 vector (Invitrogen Life Technologies) and sequenced using a Thermo Sequenase cycle sequencing kit (Amersham Biosciences).

Histochemical analysis

After Tg and wild-type mice had been sacrificed, cerebrum, cerebellum, submandibular gland, lung, kidney, liver, small intestine, colon, testis, pancreas, spleen, TA and soleus muscles, diaphragm, and heart were isolated and frozen in liquid nitrogen cooled isopentane. Cryosections (10 μm) from several tissues were stained with hematoxylin and eosin (H&E) and with 5-bromo-4-chloro-3-indolyl-β-D-galactopyranoside (X-Gal; Wako Chemicals, Japan) as described elsewhere [26].

Immunohistochemistry

Serial transverse cryosections (6 μm) from different tissues were placed on a slide, then dried and fixed in acetone for 6 min at −20 °C. We carried out immunohistochemical analysis with a rabbit polyclonal antibody against human utrophin (UT-2), which recognizes amino acid positions 1768–2078 [27]. The primary antibodies were detected with Alexa 488-labeled goat anti-rabbit IgG (Molecular Probes, USA). The nucleus was stained with TOTO-3 iodide (Molecular Probes). The NMJ was stained with Alexa 594-labeled α-bungarotoxin (α-BTX) (Molecular Probes). Signals were recorded photographically with a laser-scanning confocal imaging system (TCSSP™, Leica).

Cardiotoxin injection

To cause muscle degeneration, we injected 100 μl of cardiotoxin (CTX) of *Naja naja atra* venom (10 μM in saline, Wako Chemicals) into the right TA muscle of 5-week-old Tg mice with a 29-gauge needle. The concentration of CTX was determined according to a previous report [28]. CTX-injected Tg mice were sacrificed 1–7 days after CTX injection. The CTX-injected and contralateral non-injected TA muscles were isolated and frozen in liquid nitrogen cooled isopentane. Cryosections (10 μm) were stained with X-Gal. At the same time, serial cryosections (6 μm) were stained with UT-2 together with Alexa 594-labeled α-BTX. Total RNA was isolated from these frozen tissues.

Administration of rIL-6 to Tg/mdx mouse muscles

To investigate the effect of IL-6 on utrophin promoter A activation, we daily injected rIL-6 (800 ng in 6 μl of phosphate-buffered saline (PBS)/day) (R&D Systems, USA) for 5 days into the TA muscles of 2-week-old Tg/*mdx* mice. rIL-6-injected Tg/*mdx* mice were sacrificed 2 days after the final injection.

Results

Generation of four mouse lines with varying numbers of copies of the promoter A/nlsLacZ transgene

To investigate the utrophin promoter A activity, we first screened a 129Sv mouse genomic library and obtained a genome clone that contained the 5320-bp 5′-flanking region of the A-*utrophin* gene and exon 1A, intron 1, and exon 2. We then subcloned it into a Bluescript II vector. Subsequently, an nls-tagged *LacZ* gene was inserted downstream of the exon 2 UTR, as shown in Figure 1B. The nls was tagged to the *LacZ* gene to clarify the nuclei in which the utrophin promoter A was activated. Four transgenic F_0 'founder' mice were identified by Southern blotting using a *LacZ* probe, and four transgenic lines were established (Figure 1). The approximate number of transgene copies was determined by Southern blotting in all four lines (data not shown). Line 1 contained about 13 copies, lines 2 and 3 contained 5–6 copies, and line 4 contained 1 copy of the transgene.

mRNA levels of the transgene in several organs of Tg mice

The level of the transgene expression in several organs of Tg mice was determined by RT-PCR. Representative results from line 2 are shown in Figure 2. High levels of transgene mRNA expression were detected in liver, testis, colon, and submandibular gland. The signal was weakly detected in small intestine and lung, and an extremely low signal was detected in kidney, cerebrum, cerebellum, and TA muscle.

Determination of the 5′ end of β-gal mRNA

To investigate whether the transcription start site of the transgene corresponds to the authentic transcription start site of A-utrophin, we carried out 5′ RACE using total RNA isolated from testis of Tg mice (line 2). We obtained a single PCR product, indicative of a single transcription start site in testis (Figure 3). We sequenced the PCR product (543 bp) and confirmed the transcription start site of the transgene in testis, which was the same as that previously reported [16].

β-Gal expression in liver, testis, colon, submandibular gland, and small intestine of Tg mice

To identify the nuclei that express the transgene, cryosections were stained with X-Gal. At the same time, serial cryosections were stained with H&E or with UT-2, a polyclonal antibody against human utrophin [27] (Figure 4). UT-2 recognizes only the full-length form

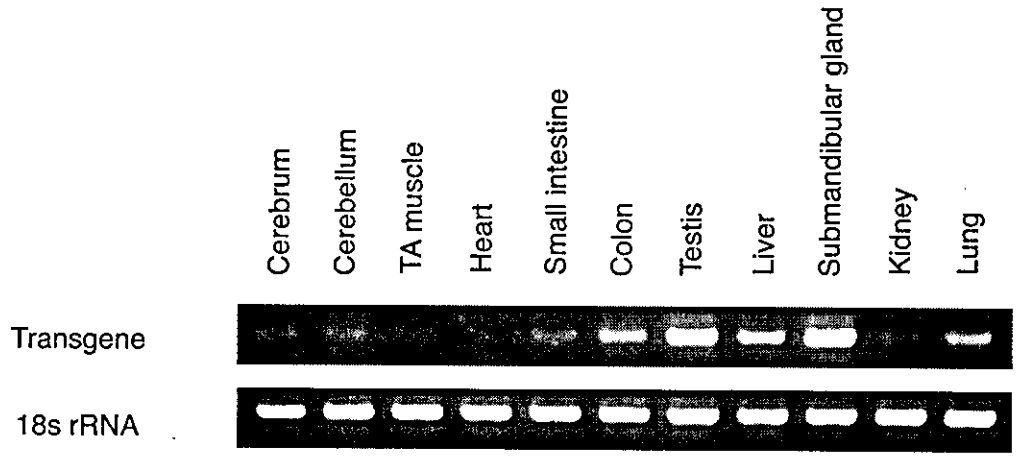

Figure 2. RT-PCR analysis of transgene mRNA from several tissues of transgenic mice. Total RNA was extracted from several tissues of 3-week-old line 2 Tg mice, and RT-PCR was performed with the transgene-specific primers described in Materials and methods. PCR products were electrophoresed on a 2% agarose gel. The expected size of the PCR product was 414 bp (transgene; *top*). As a control, 18s rRNA (297 bp; *bottom*) was co-amplified

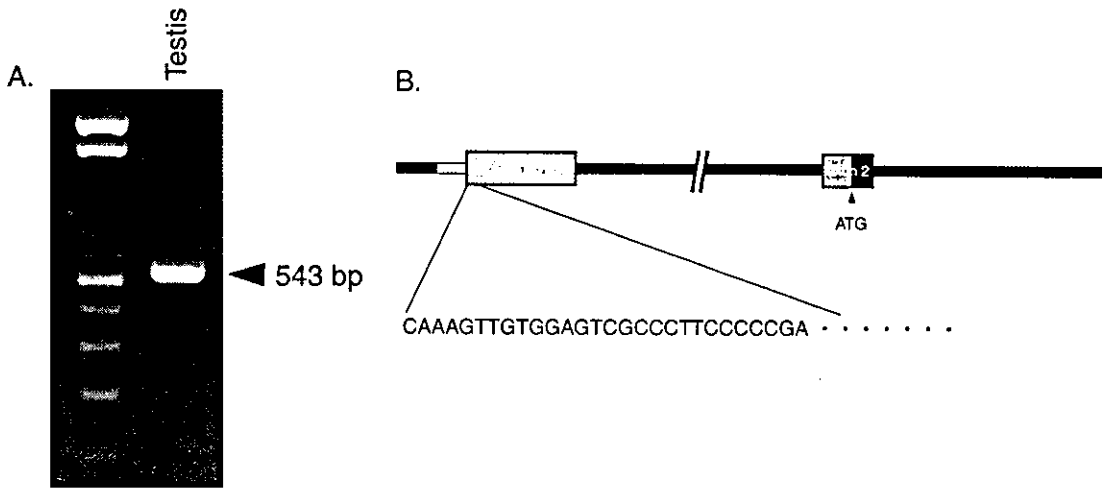

Figure 3. 5′ RACE analysis of transcription initiation sites. (A) 5′ RACE analysis with total RNA (1.5 μg) of the testis from 3-week-old line 2 Tg mice was performed using the gene-specific primers described in Materials and methods. The final PCR products were separated on a 2% agarose gel. (B) Sequencing products confirmed that the transgene was transcribed from the authentic initiation site of the utrophin A promoter (data not shown)

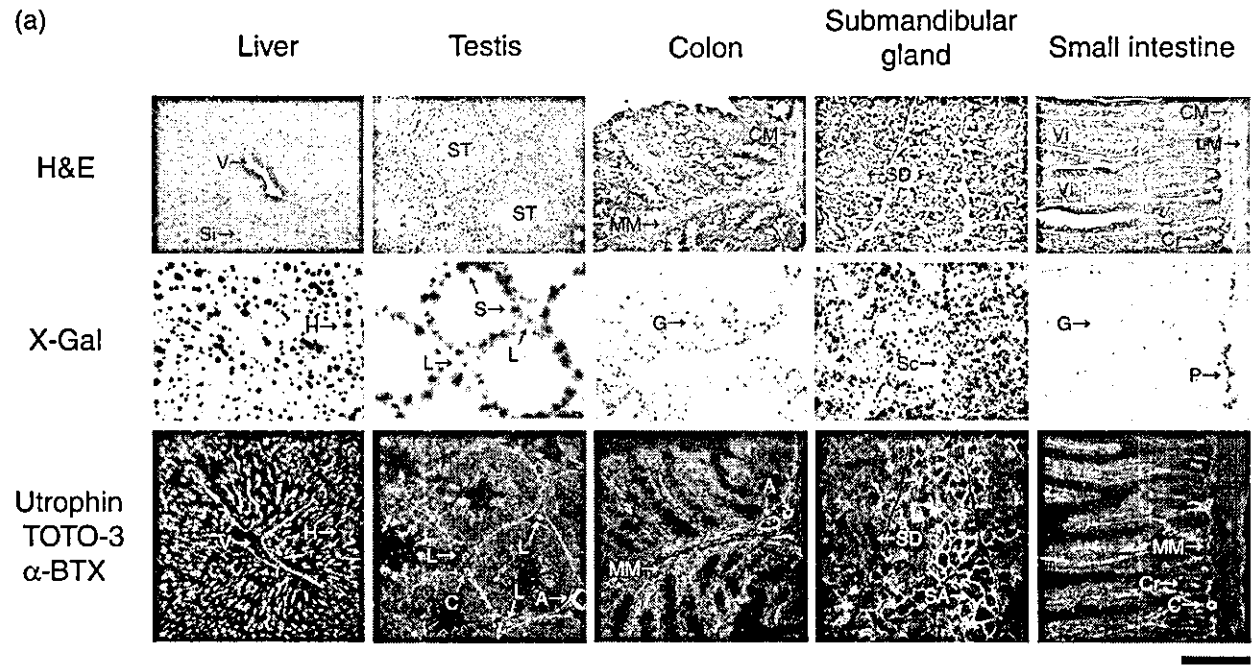

Figure 4. Histological and immunohistochemical analysis of transgenic mice. Cryosections (10 μm) were prepared from tissues (liver, testis, colon, submandibular gland, and small intestine (A), kidney and lung (B), cerebrum, cerebellum, heart, and TA muscle (C)) from 8-week-old line 2 Tg mice and stained with H&E (*top*) or X-Gal (*middle*). Serial 6 μm cryosections were stained with a polyclonal antibody against utrophin (UT-2; green). Nuclei were stained with TOTO-3 (blue). The NMJs were identified with α-BTX (red) (*bottom*). Shown are representative results obtained from line 2 Tg mice. Identical staining patterns were seen in all transgenic lines. V, terminal hepatic venule; Si, sinusoid; H, hepatocyte; ST, seminiferous tubule; L, Leydig cell; S, Sertoli cell; C, capillary; A, arteriole; MM, muscularis mucosa; CM, inner circular muscle layer; LM, outer longitudinal muscle layer; G, goblet cell; SD, striated duct; Sc, serous secretory cell; SA, serous acinus; Vi, villus; Cr, crypt; P, Paneth cell; T, cortical renal tubule; Gl, glomerulus; Al, alveolar cell; PV, pulmonary veinule; CP, choroid plexus; PM, pia mater; CC, cerebral cortex; N, neuron; ML, molecular layer; GL, granular layer; P, Purkinje cell; ID, intercalated disk; NMJ, neuromuscular junction. Bar, 100 μm

that includes both A-utrophin and B-utrophin [27]. We examined β-gal expression in all tissues in which A-utrophin has been reported to be expressed [20], and found that β-gal expression coincided well with endogenous A-utrophin expression in liver, testis, colon, submandibular gland, and small intestine.

In the liver, the nuclei of hepatocytes, but not sinusoid lining cells, were strongly stained with X-Gal, while endogenous utrophin protein was detected in the margins of hepatocytes along sinusoids and terminal hepatic venules.

In the testis, β-gal activity was found in Sertoli cells in the basal compartment of the seminiferous tubules, but not in the adluminal compartment, and in Leydig cells in the interstitial supporting tissues between the seminiferous tubules. Consistent with this observation, endogenous utrophin signals were found along the basement membrane of the seminiferous tubules and Leydig cells.

In the colon, β-gal-positive nuclei were found in goblet cells in large intestinal glands. Endogenous utrophin signals were found along the basement membrane of large intestinal glands and muscularis mucosa.

In the submandibular gland, the nuclei of both serous and mucous secretory cells were clearly stained with X-Gal. The striated duct epithelia lacked the β-gal signal. Endogenous utrophin was detected along the basement

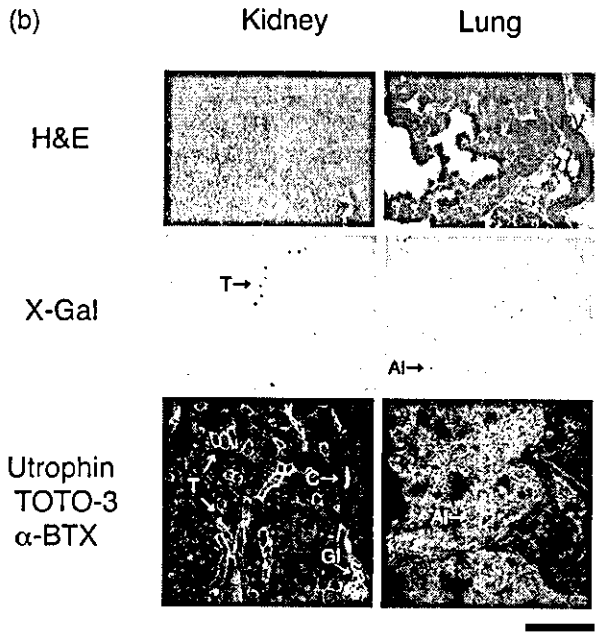

Figure 4. (*Continued*)

membrane of serous and mucous acini, but not of striated ducts.

In the small intestine, β-gal-positive nuclei were found in goblet cells and epithelia of the bases of villi and crypts.

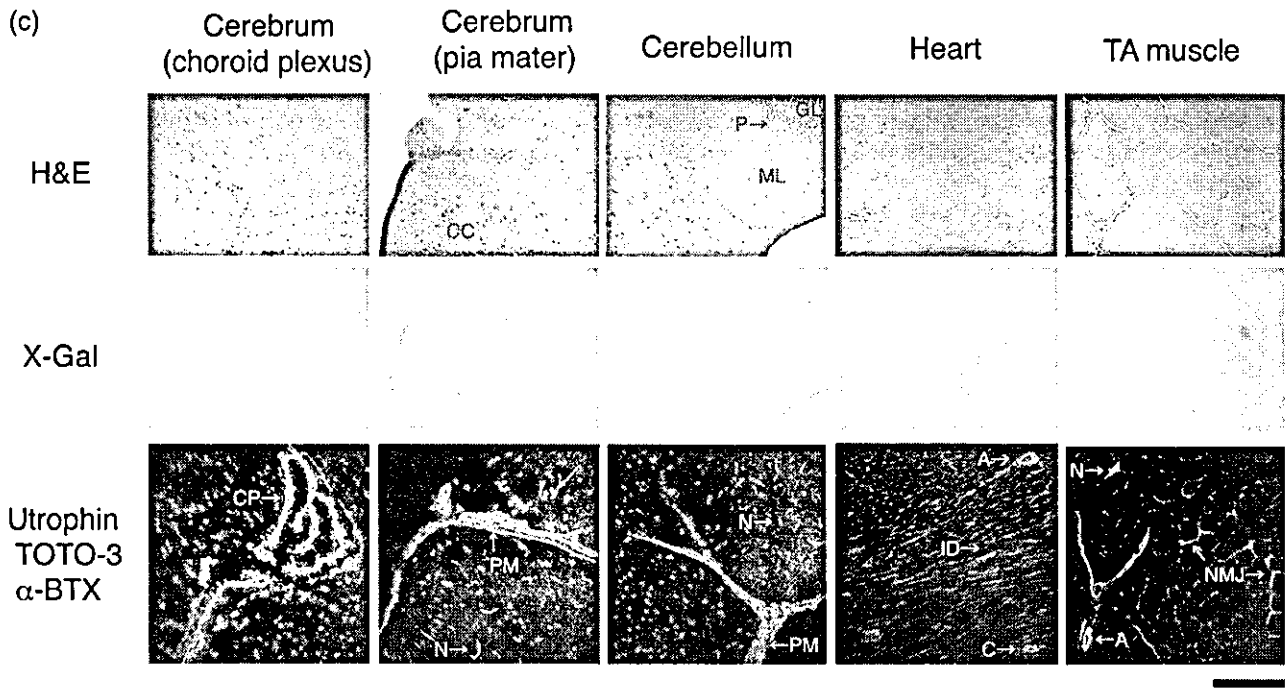

Figure 4. (*Continued*)

β-Gal signals were stronger in a subset of cells, and their characteristic distribution suggests that these cells were Paneth cells. Endogenous utrophin signals were found along the basement membrane of villi and crypts and in muscularis mucosa.

In the kidney, β-gal-positive nuclei were found in the epithelia of cortical renal tubules, but not in glomeruli. It is not clear whether β-gal-positive nuclei were present in proximal convoluted tubules, distal convoluted tubules, collecting tubules, or collecting ducts. Endogenous utrophin was found along the basement membrane of cortical renal tubules, collecting ducts of the renal medulla and Bowman's capsules, and in glomerular capillaries.

In the lung, β-gal-positive nuclei were found in alveoli, but not in terminal bronchiole epithelia. It is not clear whether β-gal-positive nuclei were present in type I or type II pneumocytes. Endogenous utrophin was found in alveolar cells and terminal bronchiole epithelia. Thus, in these tissues, endogenous utrophin protein seems to localize at the plasma membranes of cells adjacent to the basement membranes.

Inconsistent results of *LacZ* expression among the four transgenic lines

In the pancreas, β-gal-positive nuclei were clearly found in exocrine cells of lines 1 and 2, but not at all in lines 3 and 4 (data not shown). Because of this inconsistency of β-gal expression patterns among the four Tg lines, we could not determine the relationship between β-gal and endogenous utrophin expression in pancreas.

β-Gal-positive nuclei were ubiquitously found in the cerebrum of line 1, but not in other lines (Table 1). The A-utrophin protein has been shown to be expressed in the pia mater and choroid plexus of the brain [20]. Nevertheless, our results indicate that the A-utrophin promoter was not active in the pia mater and choroid plexus in our Tg mice (Figure 4C).

In the cerebellum, β-gal-positive nuclei were found in granular cells of lines 1 and 3, but not at all in lines 2 and 4 (Figure 4C, Table 1). The A-utrophin protein has been shown to be expressed in the pia mater of the cerebellum [20]. Nevertheless, our results indicate that the A-utrophin promoter was not active in the pia mater of the cerebellum in our Tg mice (Figure 4C). We speculate that this discrepancy is due to the positional effects of the transgene integration into the mouse genome.

In the spleen, β-gal-positive nuclei were not found in any of the four lines, although endogenous utrophin was found in endothelial cells of venous sinuses in red pulp (data not shown). It seems that β-gal expression was not detected in spleen of our Tg lines because B-utrophin was observed in endothelia of blood vessels [20].

β-Gal-positive nuclei were not found in cardiac, skeletal, or vascular smooth muscle

A previous study using antibodies specific to A- and B-utrophins showed that, in skeletal muscle, A-utrophin is expressed in the NMJ, peripheral nerves, and larger blood vessels [20]. However, we detected β-gal expression in neither the NMJ nor peripheral nerves of Tg skeletal muscles. As expected, β-gal expression was not found in blood vessels of Tg mouse tissues, where B-utrophin has been reported to be expressed. Unexpectedly, we did

Table 1. Summary of β-gal expression in four transgenic lines. Tg mice (lines 1–4) were sacrificed at 3 weeks old and 8 weeks old and β-gal expression in several tissues was examined. No β-gal-positive nuclei were found in non-transgenic littermates. β-Gal expression level is shown as follows: –, none; ±, trace; +, weak; ++, moderate; +++, strong

	Young (3–5w)				Adult (8–18w)			
	line 1	line 2	line 3	line 4	line 1	line 2	line 3	line 4
Cerebrum	++	–	–	–	++	–	–	–
Cerebellum	+	–	+	–	++	–	+	–
Heart	–	–	–	–	–	–	–	–
TA muscle	–	–	–	–	–	–	–	–
Soleus muscle	–	–	–	–	–	–	–	–
Diaphragm	–	–	–	–	–	–	–	–
Arteriole	–	–	–	–	–	–	–	–
Small intestine	+	+	+	–	+	+	–	–
Colon	+	++	++	++	++	++	+	+
Testis	+++	+++	++	–	+++	+++	++	–
Liver	++	++	±	±	++	+++	±	±
Submandibular gland	+++	+++	++	–	+++	+++	++	–
Kidney	+	±	±	±	±	±	–	–
Lung	++	+	–		+	+	–	–
Pancreas	++	+	–	–	++	+	–	–
Spleen	–	–	–	–	–	–	–	–

Table 2. Cells that express β-gal in transgenic mice and comparison with endogenous utrophin expression. Examined tissues were categorized into three groups. Group I: β-gal expression and endogenous utrophin expression coincide well. Group II: β-gal expression partially recapitulates endogenous utrophin expression. Group III: β-gal expression was not detected in spite of endogenous utrophin expression. The localization of endogenous utrophin is based on this study and previous studies [20]. BM, basement membrane; N.D., not detected

	Tissue	Endogenous utrophin	β-Gal expression
I	Liver	Surface of hepatocyte (space of Disse)	hepatocyte
	Testis	BM of seminiferous tubule	Sertoli cell
		Leydig cell	Leydig cell
	Colon	BM of large intestinal gland	goblet cell
		muscularis mucosa	N.D.
	Submandibular gland	BM of serous & mucous acinus	serous & mucous secretory cell
	Small intestine	BM of villus & crypt	Paneth cell, goblet cell
		muscularis mucosa	N.D.
II	Kidney	BM of cortical renal tubule	epithelial cell of cortical renal tubule
		BM of collecting duct in renal medulla	
		glomerulus	N.D.
	Lung	alveolus	alveolar cell
		terminal bronchiole epithelium	N.D.
III	Cerebrum	choroid plexus	N.D.
		pia mater	
	Cerebellum	pia mater	N.D.
	Heart	intercalated disk	N.D.
		T tubule	
	Skeletal muscle	neuromuscular junction	N.D.
		myotendinous junction	
		regenerating muscle fiber	
	Blood vessel	vascular smooth muscle	N.D.
		endothelium	
		capillary	
	Spleen	endothelial cell of venous sinus in red pulp	N.D.

not detect β-gal expression signals in Tg vascular smooth muscle. Furthermore, cardiac muscle in transgenic mice showed no β-gal-positive nuclei (Figure 4C).

β-Gal expression in the four Tg lines is summarized in Table 1. Table 2 is a comparison between β-gal expression and immunohistochemical detection of endogenous utrophin in the utrophin promoter A-*LacZ* transgenic mice. Group I consists of the tissues in which the pattern of β-gal expression corresponded well to that of endogenous utrophin. Group II includes the tissues in which β-gal-positive nuclei were found in only a few subsets of cells expressing endogenous utrophin. Group III contains the tissues in which A-utrophin is reported to be expressed [20], but β-gal expression was not detected at all.

Regenerating and *mdx* skeletal muscles show no expression of transgene

Utrophin is up-regulated in *mdx* muscle. To analyze the β-gal expression in Tg/*mdx* muscle, we mated Tg F_1 male

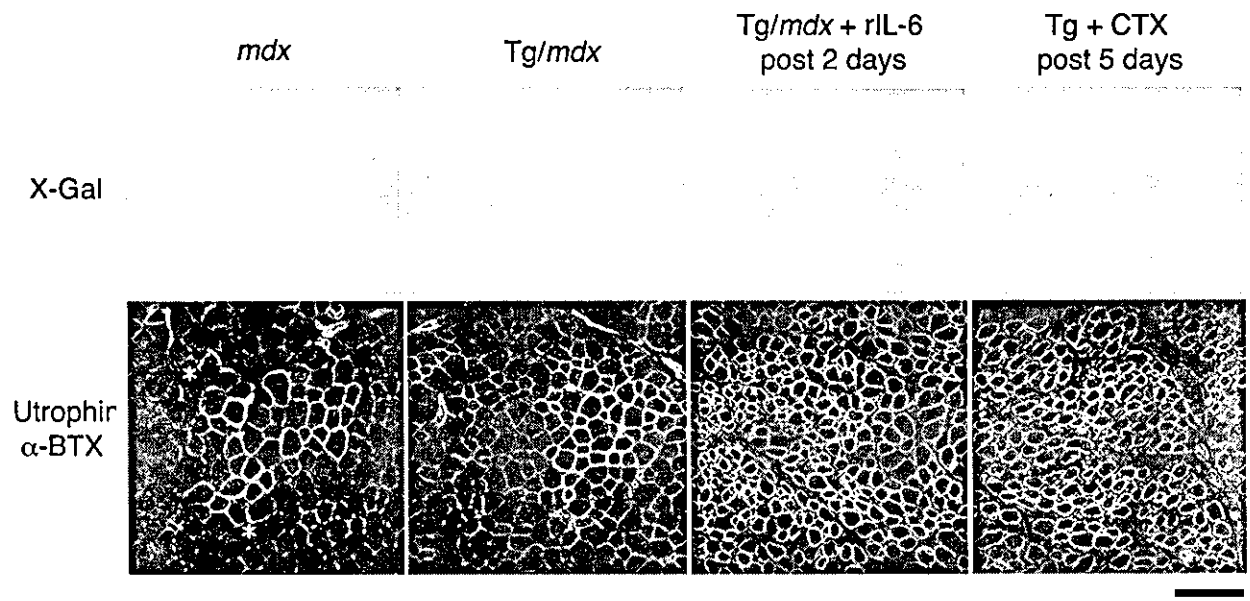

Figure 5. Effects of recombinant IL-6 and CTX injection into TA muscle of transgenic mice on transgene expression (β-gal). Cryosections of TA muscle from *mdx* mice, Tg *mdx* male mice (Tg/*mdx*), CTX-injected Tg TA muscle (Tg + CTX), and rIL-6-injected Tg *mdx* TA muscle (Tg/*mdx* + rIL-6) were stained with X-Gal (*top*) or stained with a polyclonal antibody against utrophin (UT-2) (green) and Alexa 594-labeled α-BTX (red) (*bottom*). rIL-6-injected Tg/*mdx* TA muscles were obtained 2 days after the final injection of rIL-6, and CTX-injected Tg TA muscles were obtained 5 days after CTX injection. * indicates NMJ. Bar, 100 μm

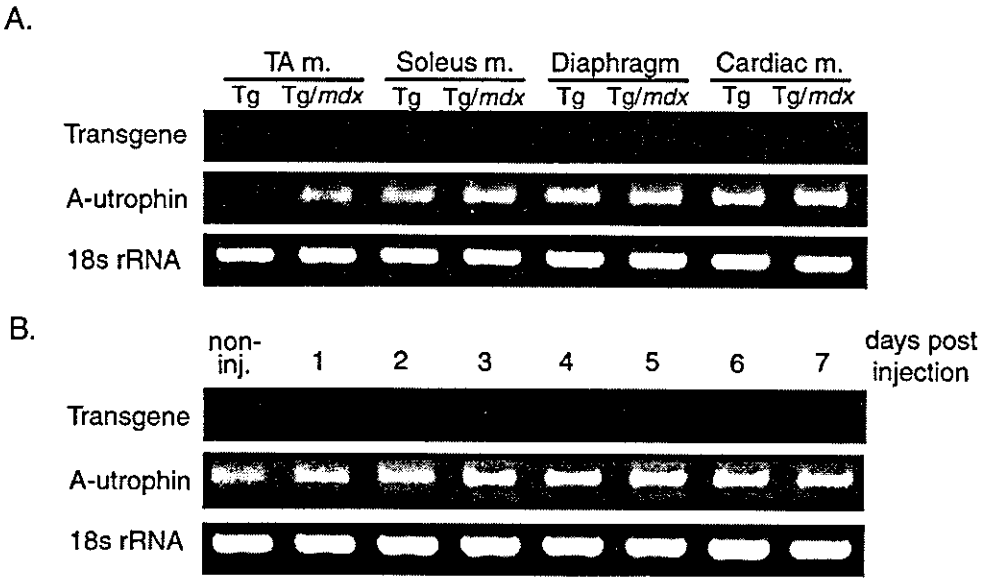

Figure 6. Effects of muscle regeneration on expression of transgene mRNA. Total RNA was extracted from TA muscle, soleus muscle, diaphragm, and cardiac muscle of 4-week-old Tg and Tg/*mdx* mice (A), and from CTX-injected 5-week-old Tg TA muscles at the indicated days after the injection (B). RT-PCR was performed with transgene-specific primers described in Materials and methods. PCR products were electrophoresed on 2% agarose gel. The expected size of PCR products was 414 bp (transgene; *top*) and 309 bp (A-utrophin; *middle*). As a control, 18s rRNA (297 bp; *bottom*) was co-amplified

mice of line 2 with *mdx* female mice (Figure 1D). Utrophin protein was overexpressed along the sarcolemma of *mdx* muscle fibers, but all myonuclei were negative for β-gal staining (Figure 5). Next, we investigated the mRNA levels of A-utrophin and transgene by RT-PCR. To this end, A-utrophin mRNA was elevated in TA muscle, soleus muscle, diaphragm, and cardiac muscle of Tg/*mdx* mice, but transgene mRNA was not detected in these muscles (Figure 6A). In addition, there was no difference in β-gal expression in various tissues other than muscle between Tg/*mdx* male mice and parental C57BL/6J-Tg mice (data not shown).

Utrophin is up-regulated in regenerating muscle. Recently, Galvagni *et al.* reported that the transcription of A-utrophin was elevated in regenerating muscle [19]. Therefore, we next injected CTX into TA muscle of line 2 Tg mice to damage muscle fibers, and analyzed β-gal expression during muscle regeneration (Figure 5).

Figure 5 shows a section of transgenic skeletal muscle isolated 5 days after CTX injection, chosen because the utrophin protein signal was detected the most strongly in it of all tissues collected after CTX injection. Utrophin was overexpressed along the sarcolemma of regenerating small muscle fibers, but all myonuclei were negative for β-gal staining. Furthermore, A-utrophin mRNA was elevated 3 days after CTX injection, but transgene mRNA was not detected in CTX-injected muscle (Figure 6B).

Administration of rIL-6 did not induce the expression of the transgene in skeletal muscle

We have previously reported that rIL-6 induced overexpression of endogenous utrophin in *mdx* skeletal muscle [24]. Subsequently, we found that rIL-6 elevated mainly A-utrophin mRNA (Itoh *et al.*, unpublished data). Therefore, we injected rIL-6 into the TA muscles of Tg/*mdx* mice daily for 5 days and analyzed the effect of rIL-6 on the transgene expression (Figure 5). Without doubt, rIL-6 induced overexpression of utrophin in Tg/*mdx* muscles, but not expression of the transgene (Figure 5). Furthermore, A-utrophin mRNA was up-regulated 2 days after the final injection, but transgene mRNA was not detected (data not shown).

Discussion

Previous transgenic studies showed that forced expression of utrophin at the sarcolemma of *mdx* muscle dramatically improved dystrophic phenotypes [11–13]. Furthermore, an adenovirally induced *utrophin* gene ameliorated the dystrophic changes in *mdx* mice [14]. On the other hand, we have previously reported that adenovirus vector-mediated expression of β-gal up-regulated endogenous utrophin at the sarcolemma in *mdx* muscle, where β-gal-positive muscle fibers were protected from the degeneration process [15]. Thus, up-regulation of utrophin stabilizes dystrophin-deficient muscle membrane and protects muscle fibers from degeneration caused by mechanical stress.

There are two full-length transcripts: A-utrophin and B-utrophin [16,17]. A-Utrophin localizes to the NMJ and in peripheral nerves [20]. The upstream promoter A is CpG-rich, TATA-less, and contains a consensus N-box, which is critical for synaptic expression of utrophin. In contrast, B-utrophin is observed in endothelial capillaries and vessels [20]. Further, A-utrophin, but not B-utrophin, is up-regulated in regenerating muscle fibers [19] or in *mdx* muscle fibers [20]. Therefore, we first examined promoter A activity using transgenic techniques. The *LacZ* gene was tagged by nls to clarify the nuclei in which promoter A is active. Contrary to our expectation, analysis of both transcripts for the transgene and β-gal staining showed that the 5320-bp 5′-flanking region of the A-*utrophin* gene is highly and constantly active in liver, testis, colon, submandibular gland, and small intestine, slightly active in kidney and lung, but not at all in striated muscles.

Intriguingly, detailed examination at the cellular level showed that promoter A is active in secretory cells. For example, in the Tg mouse liver, β-gal-positive nuclei were found in hepatocytes, which synthesize and secrete bile. In the Tg mouse testis, β-gal-positive nuclei were found in Sertoli cells and Leydig cells. Sertoli cells of the fetal testis produce and secrete Mullerian-inhibiting substance (MIS), which suppresses the development of the reproductive tract and results in regression of the Mullerian duct in the female. MIS is also produced in the adult gonads and plays a role in maintaining testosterone homeostasis [29]. Leydig cells synthesize and secrete testosterone, which induces male secondary sexual characteristics. In the Tg mouse colon, β-gal-positive nuclei were found in goblet cells, which produce mucin. In the submandibular gland, nuclei of serous or mucous secretory cells, which secrete saliva, were clearly stained with X-Gal, although the Tg mouse striated duct epithelia, which secrete lysozyme and IgA, lacked β-gal expression. In the Tg mouse small intestine, β-gal-positive nuclei were found in goblet cells and Paneth cells. Goblet cells secrete mucus, and Paneth cells secrete microbicidal α-defensins when exposed to bacteria or bacterial antigens [30]. Previous studies showed that utrophin is found at high levels in secretory tissues including pituitary, thyroid, adrenal glands, and choroid plexus epithelia, which secrete glucocorticoid hormones, the iodine-containing hormones tri-iodothyronine and thyroxine, steroid and catecholamine hormones, and cerebrospinal fluid, respectively [31,32]. We detected A-utrophin expression in the secretory cells of our Tg mice. We speculate that utrophin may have other unknown functions as well as supporting secretory cells.

In the Tg mouse kidney, endogenous utrophin was expressed in glomerular tufts, cortical renal tubules, and collecting ducts in the renal medulla, and A-utrophin protein has been shown to be expressed in glomerular tufts and tubules of the renal cortex [20]. However, β-gal signals were found in only a few epithelia of cortical renal tubules. On the other hand, endogenous utrophin signals were found along the basement membrane of cortical renal tubules, possibly assembling the DAP complex at the plasma membrane and interacting with laminin in the basement membrane. The reason β-gal-positive nuclei were not found in glomeruli is unknown. In the Tg mouse lung, a small number of β-gal-positive nuclei were found in a few type I or type II pneumocytes. The reason for this discrepancy is unclear.

In the cerebrum and the cerebellum of Tg mice, transgene mRNA was detected at extremely low levels, while β-gal-positive nuclei were not detected at all in the choroid plexus and pia mater. In these tissues, the transcriptional level was also low, and the stability of transgene mRNA may be lower than the transcriptional level, as in skeletal muscle.

In this study, unexpectedly, we detected extremely low levels of transgene mRNA in skeletal muscle and no β-gal staining in myonuclei even in the vicinity of the NMJs. Likewise, the expression of the transgene was not observed in regenerating muscle of the utrophin promoter A/*LacZ* transgenic mice. Further, we previously reported that IL-6 induced overexpression of utrophin in neonatal *mdx* muscle [24]. However, the expression of β-gal was not observed in rIL-6-injected Tg/*mdx* muscle. Briefly, the promoter of the A-*utrophin* gene is not active in cardiac and skeletal muscle, and there are several possibilities for a regulatory mechanism of A-utrophin expression in skeletal and cardiac muscle. First, the transgene construct used in this study contained the 5′-flanking region (5320 bp) of the A-*utrophin* gene, but lacked the intronic enhancer (downstream utrophin enhancer, DUE) within the second intron, which has recently been reported [18]. Therefore, it is reasonable to speculate that the intronic enhancer is indispensable for the expression of utrophin in both skeletal muscle and cardiac muscle. Second, the 5320 bp of the 5′-flanking region or first intron might contain a silencer region for the expression of A-utrophin in skeletal and cardiac muscle, since Galvagni *et al.* reported that *LacZ* expression was detected in muscle cell transfected with the promoter alone [19]. Third, important roles for the 3′-UTR of utrophin mRNA in stabilization have been suggested, and two RNA-binding proteins have been reported [22]. For example, Gramolini *et al.* reported ~42- kDa and 90-kDa proteins that bind utrophin 3′-UTR and are expressed more abundantly in extensor digitorum longus muscles than in soleus muscles. Hence, higher levels of utrophin mRNA in soleus muscles suggest that these proteins destabilize utrophin mRNA [22]. Furthermore, Gramolini *et al.* reported that the utrophin 3′-UTR is responsible for targeting utrophin mRNA to cytoskeletal-bound polysomes, binding actin, and controlling transcript stability [23]. We previously reported that adenovirus vector-mediated gene transfer into skeletal muscle evoked robust expression of endogenous utrophin via immune response [15], in which both A-utrophin and B-utrophin mRNA levels were continuously elevated (Itoh *et al.*, unpublished data). These results suggest that utrophin overexpression is induced by one or more inflammatory cytokines, and most of the effects seem to be due to post-transcriptional regulation. These observations and our results suggest that the expression of utrophin in skeletal muscle might be regulated at the post-transcriptional level via 3′-UTR. Finally, it is also important to note that the utrophin protein seems to be relatively stable at the sarcolemma in skeletal muscle [22]. Once the utrophin protein forms the dystrophin–glycoprotein complex at the sarcolemma, it might be extremely stable in muscle fibers compared with β-gal.

In summary, we showed here that the 5-kb flanking region of the A-*utrophin* gene containing the A-utrophin core promoter drives high levels of A-utrophin transcription in liver, testis, colon, submandibular gland, and small intestine, but not in skeletal and cardiac muscle, indicating that A-utrophin expression in striated muscle is greatly dependent on other regulatory elements.

Acknowledgements

We thank Dr. Hirata and Dr. Yokota for technical instructions. We also thank S. Masuda and A. Fukase for technical assistance, and colleagues in our laboratory for useful discussion and suggestions on this work. This work is supported by Grants-in-Aid for Center of Excellence (COE), Research on Nervous and Mental Disorders (10B-1, 13B-1), and Health Science Research Grants for Research on the Human Genome and Gene Therapy (H10-genome-015, H13-genome-001), for Research on Brain Science (H12-Brain-028, H15-Brain-021) from the Ministry of Health, Labor and Welfare, Grants-in Aids for Scientific Research (10 557 065, 11 470 153, 11 170 264, 14 657 158 and 15 390 281) from the Ministry of Education, Culture, Sports, Science and Technology, and a Research Grant from the Human Frontier Science Project.

References

1. Koenig M, Hoffman EP, Bertelson CJ, *et al.* Complete cloning of the Duchenne muscular dystrophy (DMD) cDNA and preliminary genomic organization of the DMD gene in normal and affected individuals. *Cell* 1987; 50: 509–517.
2. Ahn AH, Kunkel LM. The structural and functional diversity of dystrophin. *Nat Genet* 1993; 3: 283–291.
3. Tinsley JM, Blake DJ, Zuellig RA, *et al.* Increasing complexity of the dystrophin-associated protein complex. *Proc Natl Acad Sci U S A* 1994; 91: 8307–8313.
4. Campbell KP. Three muscular dystrophies: loss of cytoskeleton-extracellular matrix linkage. *Cell* 1995; 80: 675–679.
5. Ozawa E, Yoshida M, Suzuki A, *et al.* Dystrophin-associated proteins in muscular dystrophy. *Hum Mol Genet* 1995; 4: 1711–1716.
6. Pearce M, Blake DJ, Tinsley JM, *et al.* The utrophin and dystrophin genes share similarities in genomic structure. *Hum Mol Genet* 1993; 2: 1765–1772.
7. Grady RM, Teng H, Nichol MC, *et al.* Skeletal and cardiac myopathies in mice lacking utrophin and dystrophin: a model for Duchenne muscular dystrophy. *Cell* 1997; 90: 729–738.
8. Khurana TS, Watkins SC, Chafey P, *et al.* Immunolocalization and developmental expression of dystrophin related protein in skeletal muscle. *Neuromuscul Disord* 1991; 1: 185–194.
9. Ohlendieck K, Ervasti JM, Matsumura K, *et al.* Dystrophin-related protein is localized to neuromuscular junctions of adult skeletal muscle. *Neuron* 1991; 7: 499–508.
10. Wilson LA, Cooper BJ, Dux L, *et al.* Expression of utrophin (dystrophin-related protein) during regeneration and maturation of skeletal muscle in canine X-linked muscular dystrophy. *Neuropathol Appl Neurobiol* 1994; 20: 359–367.
11. Tinsley JM, Potter AC, Phelps SR, *et al.* Amelioration of the dystrophic phenotype of mdx mice using a truncated utrophin transgene. *Nature* 1996; 384: 349–353.
12. Deconinck N, Tinsley JM, De Backer F, *et al.* Expression of truncated utrophin leads to major functional improvements in dystrophin-deficient muscles of mice. *Nat Med* 1997; 3: 1216–1221.
13. Tinsley JM, Deconinck N, Fisher R, *et al.* Expression of full-length utrophin prevents muscular dystrophy in mdx mice. *Nat Med* 1998; 4: 1441–1444.
14. Gilbert R, Nalbantoglu J, Petrof BJ, *et al.* Adenovirus-mediated utrophin gene transfer mitigates the dystrophic phenotype of mdx mouse muscles. *Hum Gene Ther* 1999; 10: 1299–1310.
15. Yamamoto K, Yuasa K, Miyagoe Y, *et al.* Immune response to adenovirus-delivered antigens upregulates utrophin and results in mitigation of muscle pathology in mdx mice. *Hum Gene Ther* 2000; 11: 669–680.
16. Dennis CL, Tinsley JM, Deconinck AE, *et al.* Molecular and functional analysis of the utrophin promoter. *Nucleic Acids Res* 1996; 24: 1646–1652.

17. Burton EA, Tinsley JM, Holzfeind PJ, *et al.* A second promoter provides an alternative target for therapeutic up-regulation of utrophin in Duchenne muscular dystrophy. *Proc Natl Acad Sci U S A* 1999; **96**: 14025–14030.
18. Galvagni F, Oliviero S. Utrophin transcription is activated by an intronic enhancer. *J Biol Chem* 2000; **275**: 3168–3172.
19. Galvagni F, Cantini M, Oliviero S. The utrophin gene is transcriptionally up-regulated in regenerating muscle. *J Biol Chem* 2002; **277**: 19106–19113.
20. Weir AP, Burton EA, Harrod G, *et al.* A- and B-utrophin have different expression patterns and are differentially up-regulated in mdx muscle. *J Biol Chem* 2002; **277**: 45285–45290.
21. Jimenez-Mallebrera C, Davies KE, Putt W, *et al.* A study of short utrophin isoforms in mice deficient for full-length utrophin. *Mamm Genome* 2003; **14**: 47–60.
22. Gramolini AO, Belanger G, Thompson JM, *et al.* Increased expression of utrophin in a slow vs. a fast muscle involves posttranscriptional events. *Am J Physiol Cell Physiol* 2001; **281**: C1300–C1309.
23. Gramolini AO, Belanger G, Jasmin BJ. Distinct regions in the 3′ untranslated region are responsible for targeting and stabilizing utrophin transcripts in skeletal muscle cells. *J Cell Biol* 2001; **154**: 1173–1183.
24. Fujimori K, Itoh Y, Yamamoto K, *et al.* Interleukin-6 induces overexpression of the sarcolemmal utrophin in neonatal mdx skeletal muscle. *Hum Gene Ther* 2002; **13**: 509–518.
25. Kalderon D, Roberts BL, Richardson WD, *et al.* A short amino acid sequence able to specify nuclear location. *Cell* 1984; **39**: 499–509.
26. Ishii A, Hagiwara Y, Saito Y, *et al.* Effective adenovirus-mediated gene expression in adult murine skeletal muscle. *Muscle Nerve* 1999; **22**: 592–599.
27. Imamura M, Ozawa E. Differential expression of dystrophin isoforms and utrophin during dibutyryl-cAMP-induced morphological differentiation of rat brain astrocytes. *Proc Natl Acad Sci U S A* 1998; **95**: 6139–6144.
28. Couteaux R, Mira JC, d'Albis A. Regeneration of muscles after cardiotoxin injury. I. Cytological aspects. *Biol Cell* 1988; **62**: 171–182.
29. Teixeira J, Fynn-Thompson E, Payne AH, *et al.* Mullerian-inhibiting substance regulates androgen synthesis at the transcriptional level. *Endocrinology* 1999; **140**: 4732–4738.
30. Ayabe T, Satchell DP, Wilson CL, *et al.* Secretion of microbicidal alpha-defensins by intestinal Paneth cells in response to bacteria. *Nat Immunol* 2000; **1**: 113–118.
31. Schofield J, Houzelstein D, Davies K, *et al.* Expression of the dystrophin-related protein (utrophin) gene during mouse embryogenesis. *Dev Dyn* 1993; **198**: 254–264.
32. Knuesel I, Bornhauser BC, Zuellig RA, *et al.* Differential expression of utrophin and dystrophin in CNS neurons: an in situ hybridization and immunohistochemical study. *J Comp Neurol* 2000; **422**: 594–611.

doi:10.1016/j.ymthe.2004.07.025

ARTICLE

AAV Vector-Mediated Microdystrophin Expression in a Relatively Small Percentage of *mdx* Myofibers Improved the *mdx* Phenotype

Madoka Yoshimura,[1,2] Miki Sakamoto,[1] Madoka Ikemoto,[1] Yasushi Mochizuki,[1] Katsutoshi Yuasa,[1] Yuko Miyagoe-Suzuki,[1] and Shin'ichi Takeda[1,*]

[1]*Department of Molecular Therapy, National Institute of Neuroscience, National Center of Neurology and Psychiatry, 4-1-1 Ogawa-higashi, Kodaira, Tokyo 187-8502, Japan*
[2]*Department of Neurology, Division of Neuroscience, Graduate School of Medicine, University of Tokyo, Hongo 7-3-1, Tokyo 113-8655, Japan*

**To whom correspondence and reprint requests should be addressed. Fax: +81 42 346 1750. E-mail: takeda@ncnp.go.jp.*

Available online 19 August 2004

Duchenne muscular dystrophy (DMD) is a lethal disorder of skeletal muscle caused by mutations in the *dystrophin* gene. Adeno-associated virus (AAV) vector-mediated gene therapy is a promising approach to the disease. Although a rod-truncated microdystrophin gene has been proven to ameliorate dystrophic phenotypes, the level of microdystrophin expression required for effective gene therapy by an AAV vector has not been determined yet. Here, we constructed a recombinant AAV type 2 vector, AAV2-MCKΔCS1, expressing microdystrophin (ΔCS1) under the control of a muscle-specific MCK promoter and injected it into TA muscles of 10-day-old and 5-week-old *mdx* mice. AAV2-MCKΔCS1-mediated gene transfer into 5-week-old *mdx* muscle resulted in extensive and long-term expression of microdystrophin and significantly improved force generation. Interestingly, 10-day-old injected muscle expressed microdystrophin in a limited number of myofibers but showed hypertrophy of microdystrophin-positive muscle fibers and considerable recovery of contractile force. Thus, we concluded that AAV2-MCKΔCS1 could be a powerful tool for gene therapy of DMD.

Key Words: Duchenne muscular dystrophy, gene therapy, adeno-associated virus vector, dystrophin, microdystrophin, skeletal muscle, *mdx* mouse, hypertrophy

INTRODUCTION

Duchenne muscular dystrophy (DMD) is an X-linked, lethal disorder of skeletal muscle caused by mutations in the *dystrophin* gene. There is no effective treatment for the disease at present, although gene therapy could be an attractive approach to the disease.

Several methods of gene transfer have been tried for the treatment of dystrophin-deficient muscular dystrophy: naked plasmid injection [1], full-length dystrophin cDNA transfer via a gutted adenovirus vector [2,3], forced splicing using oligonucleotides [4], and gene repair by a chimeric RNA/DNA oligonucleotide [5]. Among several gene transfer methods, an adeno-associated virus (AAV) vector-mediated gene transfer is one of the most promising approaches to DMD because AAV vectors have been shown to evoke minimal immune responses and mediate long-term transgene expression in skeletal muscle [6–8]. Since the capacity of an AAV vector to incorporate an exogenous gene is limited to 4.9 kb, several groups have attempted to truncate the 14-kb dystrophin cDNA to obtain functional microdystrophins to be inserted into AAV vectors [9–13]. We previously constructed three rod-truncated microdystrophins and generated transgenic *mdx* mice expressing these microdystrophins. Among the three microdystrophins tested, only the 4.9-kb microdystrophin CS1 completely prevented muscle degeneration of dystrophin-deficient *mdx* mice [14]. Based on this result, we generated an AAV vector carrying ΔCS1 microdystrophin cDNA, a modified version of CS1 cDNA, and injected the vectors (designated AAV2-MCKΔCS1) directly into both 10-day-old and 5-week-old *mdx* muscles. In this study, we demonstrate that AAV vector-injected *mdx* muscles showed functional recovery even 24 weeks after treatment. Surprisingly, when introduced into neonatal muscle, microdystrophin expression in a relatively small percentage of

1525-0016/$30.00

doi:10.1016/j.ymthe.2004.07.025

muscle fibers dramatically improved the contractile properties of dystrophic muscle. This improvement in contractile force was thought to be achieved by hypertrophied microdystrophin-positive muscle fibers.

RESULTS

Construction of an AAV-2 Vector Carrying Microdystrophin ΔCS1

We constructed an AAV-2 vector encoding microdystrophin ΔCS1 under the control of a truncated, muscle-specific creatine kinase (MCK) promoter [15]. We designated this recombinant AAV vector AAV2-MCKΔCS1. CS1, which has the N-terminal, actin-binding domain, four rod repeats and three hinges, the cysteine-rich domain, and the C-terminal domain, effectively rescued dystrophic phenotypes when introduced as a transgene [14]. To shorten CS1 cDNA (4.9 kb) further, we deleted the 5′ and 3′ untranslated regions (UTRs) and exons 71–78 (alternative splicing regions of dystrophin mRNA) by PCR techniques. We named the resultant 3.8-kb cDNA ΔCS1 (Fig. 1).

Expression of ΔCS1 Microdystrophin at the Sarcolemma after AAV2-MCKΔCS1-Mediated Gene Transfer into *mdx* Muscle

We injected AAV2-MCKΔCS1 into tibialis anterior (TA) muscles of 10-day-old and 5-week-old dystrophin-deficient *mdx* mice (7.5×10^{10} vector genomes (vg) for neonatal muscle; 2.5×10^{11} vg for young muscle). In a natural course, 10-day-old *mdx* muscle shows no obvious dystrophic changes, while 5-week-old *mdx* muscle shows active cycles of the degeneration–regeneration process. We also analyzed contralateral TA muscles from the treated *mdx* mice and TA muscles from age-matched C57BL/10 (B10) mice as controls. When examined at 8 and 24 weeks after AAV2-MCKΔCS1 injection, ΔCS1 had correctly localized at the sarcolemma (Figs. 2A and 2C). Western blot using a dystrophin antibody showed a band of the expected size (138 kDa) in the AAV vector-injected *mdx* muscles (Fig. 2G). Most of the ΔCS1-positive fibers were peripherally nucleated when AAV2-MCKΔCS1 was injected into 10-day-old *mdx* muscles (Figs. 2A and 2B). In contrast, we observed both centrally and peripherally nucleated fibers when the vectors were injected into 5-week-old *mdx* muscle (Figs. 2C and 2D). The mean percentages of ΔCS1-positive fibers were 22.2 ± 11.4% at 8 weeks and 16.5 ± 7.0% at 24 weeks after injection at 10 days of age (Fig. 2E). When injected at 5 weeks of age, the mean percentages of dystrophin-positive fibers were 39.2 ± 15.8% at 8 weeks and 51.5 ± 17.3% at 24 weeks after vector injection (Fig. 2F). Next, we quantified the amount of ΔCS1 protein by immunoblotting. The amount of microdystrophin protein in the AAV-injected *mdx* muscles at 10 days of age was 12.7 ± 8.4% of that of full-length dystrophin in B10 muscle at 8 weeks (data not shown) and 9.2 ± 1.4% at 24 weeks after injection (Fig. 2G). When we injected AAV2-MCKΔCS1 into 5-week-old *mdx* muscles, the amount was 32.6 ± 8.0% of that of B10 muscle at 8 weeks and 39.8 ± 7.0% at 24 weeks after injection (data not shown).

AAV Vector-Mediated ΔCS1 Expression Ameliorated Dystrophic Phenotypes at 24 Weeks after Injection

When we analyzed *mdx* muscles treated at 10 days of age at 24 weeks after vector injection, only a small percentage of the ΔCS1-positive fibers (12.5 ± 7.8%) had central nuclei compared with untreated *mdx* muscle fibers (Fig. 3A), suggesting the protective function of ΔCS1 against muscle degeneration. In contrast, the percentage of

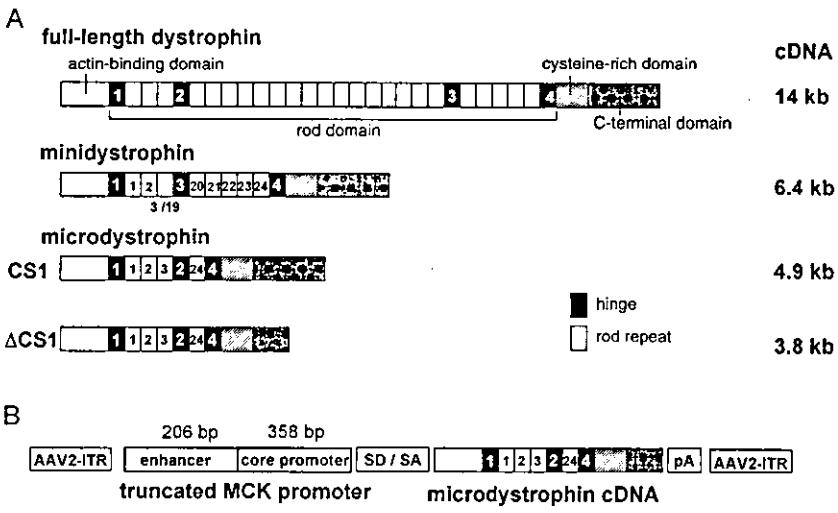

FIG. 1. Diagrams of human full-length dystrophin, minidystrophin, and microdystrophin cDNAs (CS1, ΔCS1) and AAV2-MCKΔCS1. (A) Full-length dystrophin has the N-terminal, actin-binding domain, central rod domain with 24 rod repeats and four hinges, cysteine-rich domain, and C-terminal domain. Minidystrophin, which was cloned from a mild Becker patient and reported previously, is shown as a reference [28]. CS1 has the N-terminal domain, a shortened version of the central rod domain with 4 rod repeats and three hinges, the cysteine-rich domain, and the C-terminal domain [14]. To incorporate microdystrophin CS1 cDNA into the AAV2 vector plasmid, we deleted the 3′ and 5′ untranslated regions and exons 71–78 from CS1 cDNA. The resultant ΔCS1 cDNA is 3.8 kb long. The number of the rod repeats or hinges is shown inside the squares. (B) Structure of the AAV2 vector expressing ΔCS1. ΔCS1 cDNA was incorporated into the AAV2 vector plasmid downstream of the truncated muscle-specific MCK promoter [15].

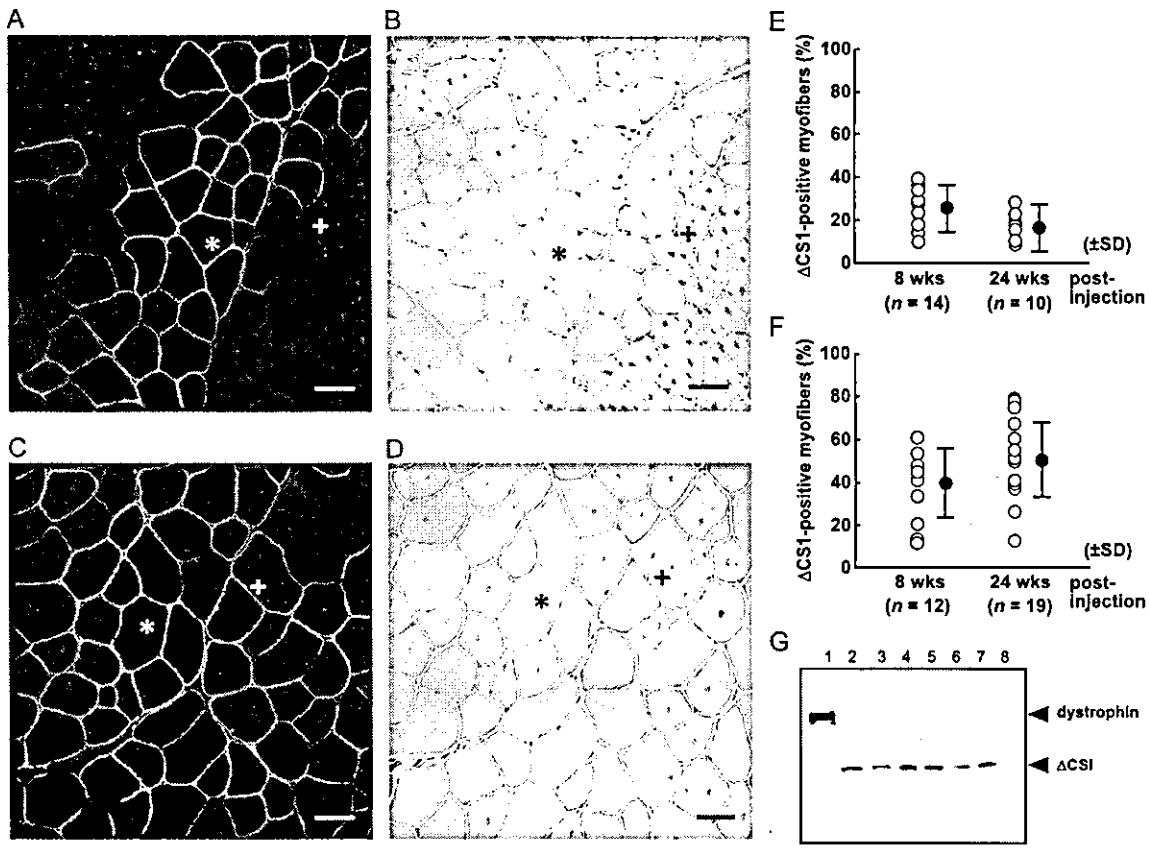

FIG. 2. ΔCS1 expression after AAV vector-mediated gene transfer into skeletal muscles of dystrophin-deficient *mdx* mice. AAV2-MCKΔCS1 was injected into TA muscles of *mdx* mice at (A, B, E) 10 days or at (C, D, F) 5 weeks of age and the muscles were analyzed at 8 or 24 weeks after injection. (A–D) Histological analysis of AAV-injected muscles 24 weeks after AAV injection. Immunofluorescence using a dystrophin antibody (A, C) and H&E staining of serial sections (B, D) is shown. ΔCS1 is correctly localized at the sarcolemma (A, C). Most ΔCS1-positive fibers (•) showed peripherally located nuclei, and their fiber diameters were relatively larger than ΔCS1-negative fibers (+) in the muscles injected at 10 days of age (A, B). In contrast to the muscles injected at the neonatal stage, many centrally nucleated fibers (+) coexist with peripherally nucleated fibers (•) in the muscles injected with the AAV vectors at 5 weeks of age (D). In (A and C), nuclei were stained with TOTO-3 (blue). Bar, 50 μm. (E, F) The percentage of ΔCS1-positive fibers among all fibers of the injected *mdx* muscle. The means (black circles) are indicated ± SD (bars). The percentage of ΔCS1-positive fibers in muscles injected at 5 weeks of age (F) was higher than in the muscles injected at 10 days of age (E). (G) Western blot analysis using a dystrophin antibody of AAV-injected *mdx* muscles. Muscles treated at 10 days of age were analyzed at 24 weeks after injection. Lane 1, C57BL/10 muscle; lanes 2–7, AAV vector-injected *mdx* muscles; lane 8, uninjected *mdx* muscle. Full-length dystrophin (lane 1) and ΔCS1 (lanes 2–7) were detected at the predicted sizes (427 or 138 kDa, respectively).

centrally nucleated fibers among ΔCS1-positive fibers in *mdx* muscles treated at 5 weeks of age (51.5 ± 11.0%) was higher than that of *mdx* muscles treated at 10 days of age (Fig. 3B).

Next, we evaluated the contractile properties of AAV2-MCKΔCS1-injected *mdx* muscle. Untreated *mdx* muscle showed remarkable hypertrophy, but its specific force was much lower than in control B10 muscle (Table 1). Similarly, the wet weight of *mdx* TA muscles treated with AAV2-MCKΔCS1 at 10 days of age was much heavier than that of control B10 TA muscles, but importantly, the maximal force was also increased (Table 1). As a result, there was no statistical difference in specific tetanic force between AAV2-MCKΔCS1-treated *mdx* muscles and age-matched B10 muscles (Table 1).

The transduction efficiency of AAV2 vector-mediated gene transfer into 10-day-old *mdx* mice was relatively low (only up to 20% of positive fibers) (Fig. 2E) compared to gene transfer into 5-week-old *mdx* mice (around 50%) (Fig. 2F), but, surprisingly, the specific tetanic force at 24 weeks after vector injection was almost equivalent to that of age-matched B10 mice and much higher than that of untreated *mdx* muscle (Table 1). To clarify the mechanism of force generation recovery by small percentages of ΔCS1-positive fibers, we next examined the relationship between muscle hypertrophy and force generation. We found a positive correlation ($r = 0.779$, $P < 0.05$) between the wet weight of the AAV2-MCKΔCS1-injected TA muscle and the force generation (Fig. 4A), but not between the muscle weight and the relative interstitial

doi:10.1016/j.ymthe.2004.07.025

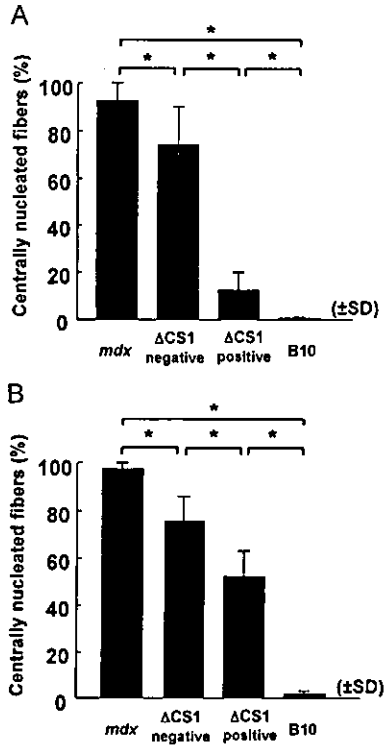

FIG. 3. Microdystrophin ΔCS1 prevents muscle degeneration. Quantitative analysis of centrally nucleated fibers among ΔCS1-positive and -negative fibers in AAV-injected *mdx* muscle. AAV2-MCKΔCS1 was injected into TA muscles of *mdx* mice at (A) 10 days or at (B) 5 weeks of age and analyzed at 24 weeks after injection. Uninjected *mdx* and age-matched control B10 muscles were also examined. (A, B) Most of the ΔCS1-positive fibers in muscles injected at 10 days of age have peripherally located nuclei (A). The percentage of centrally nucleated fibers in ΔCS1-positive fibers in muscles treated at 5 weeks of age (51.5 ± 11.0%) (B) was higher than that in muscles treated at 10 days of age (12.5 ± 7.8%) (A). Note that the ratio of centrally nucleated fibers was significantly reduced even in ΔCS1-negative fibers in muscles injected at both ages. *$P < 0.01$.

area ($r = -0.596$, $P > 0.05$) (Fig. 4B). To confirm whether increased muscle weight reflected myofiber hypertrophy, we measured individual cross-sectional areas (CSAs) of ΔCS1-positive or -negative myofibers in AAV-injected *mdx* muscles. The mean value of fiber CSAs was remarkably larger in ΔCS1-positive *mdx* fibers than in B10 fibers (Fig. 4C). Histogram analysis further demonstrated that the fiber CSA distribution of ΔCS1-positive *mdx* fibers was shifted to the right compared to that of B10 muscle; larger caliber fibers were dominant, reflecting hypertrophy of ΔCS1-expressing fibers (Fig. 4E). Thus, hypertrophied ΔCS1-positive fibers seemed to greatly improve contractile force generation. Some of the untreated and ΔCS1-negative *mdx* fibers were also hypertrophied, but the hypertrophied fibers seemed not to improve the specific force (Fig. 4E).

When we injected 5-week-old mice, force generation was recovered in AAV-injected *mdx* muscles, as when we treated 10-day-old mice, but there was no statistically significant difference in muscle weight between AAV-treated *mdx* muscles and B10 muscles (Table 1). The muscle weight had no correlation with the force generation ($r = -0.512$, $P > 0.05$) (data not shown). In addition, hypertrophy of ΔCS1-positive fibers was not obvious (Fig. 4D). Therefore, we concluded that improved specific force of the *mdx* muscles treated at 5 weeks of age was achieved without hypertrophy, possibly because approximately 50% of the muscle fibers were fully functional for ΔCS1 expression.

DISCUSSION

The level of dystrophin or minidystrophin expression required for effective gene therapy has not been determined yet, although estimates based on either transgenic *mdx* mouse studies [16–18] or the analysis of asymptomatic carriers of dystrophin-deficiency have been reported [19]. Clerk et al. reported that immunostaining showed very few dystrophin-negative fibers in muscles of asymptomatic DMD carriers, while immunoblot analysis revealed a considerable reduction in dystrophin [19]. Furthermore, it was reported that transgenic *mdx* mice expressing a minidystrophin at only 20–30% of endogenous dystrophin levels showed significantly reduced myopathic phenotypes [17]. Phelps et al. suggested that uniform expression of dystrophin is much more beneficial than the variable pattern when the overall levels of dystrophin expression were the same [18]. These findings suggest that the percentage of dystrophin-expressing fibers is more critical than the total amount of the protein. On the other hand, Rafael *et al.* showed that the expression of minidystrophin in only half the *mdx* muscle fibers resulted in a markedly milder phenotype than *mdx* mice showed [16], suggesting that dystrophin-positive fibers rescue surrounding dystrophin-negative fibers from degenerative changes. In this study, we administrated a recombinant AAV vector containing a human microdystrophin gene to the *mdx* muscle and analyzed the relationship between the level or extent of microdystrophin expression and the recovery of contractile force. Importantly, relatively small percentages of muscle fibers (less than 20%) dramatically improved the specific contractile force of dystrophic muscle. Although the molecular mechanisms by which microdystrophin recovers the specific contractile force remain to be shown, this result is encouraging in that the function of dystrophin-deficient muscle might be greatly improved by fewer dystrophin-positive myofibers than previously estimated. As shown in Fig. 3, however, there is a significant reduction in the percentage of centrally nucleated fibers among ΔCS1-negative *mdx* fibers compared to untreated *mdx* muscle, suggesting that microdystrophin expression at levels below the detection limits of immunostaining might be partially protective. There-

TABLE 1: Contractile properties of AAV2-MCKΔCS1-injected *mdx* muscle

	Muscle length (L_0, mm)	Muscle weight (MW, mg)	Maximal force (P_0, mN)	Specific force[a] (mN/mm^2)
		Injection at 10 days of age		
B10 (n = 4)	16.1 ± 0.9	48.7 ± 2.8	91.3 ± 18.1	32.0 ± 5.9
AAV-*mdx* (n = 7)	16.1 ± 1.2	64.3 ± 4.7*,**	116.5 ± 29.9**	30.9 ± 7.9**
mdx (n = 7)	16.1 ± 1.0	70.9 ± 7.0*	79.8 ± 20.0	19.1 ± 3.8*
		Injection at 5 weeks of age		
B10 (n = 6)	15.8 ± 0.9	54.9 ± 5.7	69.0 ± 31.0	20.9 ± 9.0
AAV-*mdx* (n = 11)	15.3 ± 0.8	60.9 ± 6.8	81.7 ± 24.2**	22.3 ± 8.2**
mdx (n = 11)	15.7 ± 0.7	67.9 ± 7.6*	42.2 ± 26.1	10.9 ± 7.5*

Force generation was measured 24 weeks after injection. Data are expressed as means ± SD.

[a] Specific force = ($P_0 \times L_0 \times 1.06$)/MW.

* Significant difference ($P < 0.05$) compared to B10.

** Significant difference ($P < 0.05$) compared to *mdx* muscles.

fore, exact estimation of the percentage of microdystrophin-positive fibers required for the full amelioration is somewhat difficult.

Recovery of absolute maximal force and specific tetanic force is one of the barometers of amelioration. The difference between the contractile properties of ΔCS1-expressing hypertrophied muscle and those of hypertrophied *mdx* muscle by overexpression of IGF-1 [20,21] deserves attention: ΔCS1-positive *mdx* muscle showed considerable recovery of specific force, whereas IGF-mediated hypertrophy modestly restored specific force and the muscle remained susceptible to damage. Similarly, a myostatin blockade of treated *mdx* muscle reportedly improved specific force to some extent, but showed a decrease in ECC force to the same extent as control *mdx* muscle [22]. For comparison of the effects of these different approaches toward DMD therapy, the resistance of ΔCS1-treated muscle to eccentric contraction remains to be evaluated. Importantly, however, myostatin antibody-treated mice showed significantly decreased serum creatine kinase concentrations, suggesting that myostatin blockade endowed dystrophin-deficient fibers with membrane stability.

Positive correlation between muscle wet weight and specific tetanic force indicates that muscle hypertrophy is responsible for functional amelioration at 10-day-old injected *mdx* mice. However, lack of small-caliber, presumably regenerative fibers is the most prominent finding on histograms of ΔCS1-positive *mdx* muscles injected at 10 days of age. Therefore, not only a mild increase in hypertrophic fibers, but also a decrease in small-sized fibers due to inhibition of the cycle of degeneration/regeneration, could greatly contribute to normalization of specific tetanic force. Reduction in embryonic myosin heavy chain and increase in mature myosin heavy chain might contribute to the functional recovery.

Watchko *et al.* injected an AAV2 vector carrying microdystrophin into *mdx* mice and observed incomplete recovery of specific tetanic force with 30–60% of dystrophin-positive fibers [13]. Their microdystrophin was slightly longer than our ΔCS1, it had three hinges, and the C-terminal domain was also deleted. Subtle differences in the construction could affect the functional aspects, and therefore we think that a functional examination of transgenic *mdx* is inevitable.

We also injected AAV2-MCKΔCS1 into 5-week-old *mdx* muscles, which usually show active cycles of muscle degeneration and regeneration. Dystrophin staining revealed that approximately 50% of *mdx* myofibers expressed human-type ΔCS1 microdystrophin 24 weeks after injection. There was no obvious sign of an immune response (data not shown). In contrast to neonatal muscle, *mdx* muscles treated at 5 weeks of age were not hypertrophied but still generated improved contractile force, indicating that widely expressed ΔCS1 could recover muscle function of adult mice without compensatory hypertrophy. Importantly, the CSAs of ΔCS1-positive fibers treated at a neonatal stage were larger than those of ΔCS1-positive fibers treated at 5 weeks of age (Figs. 4C and 4D). One possible explanation for this is that neonatal muscle has a high potency of compensatory hypertrophy in response to force deficit.

Our ΔCS1 and R4-R23/delta71-78, previously reported by Harper et al. [11], have similar structures. R4-R23/delta71-78 robustly transformed centrally nucleated fibers into peripherally nucleated fibers [11]. In contrast, the expression of ΔCS1 in adult *mdx* myofibers resulted in a modest reduction of centrally nucleated fibers when introduced into 5-week-old *mdx* muscle (Fig. 3B). A possible explanation for this discrepancy is a difference in the promoters that drive the microdystrophin expression. Harper *et al.* used a muscle-specific, potent promoter, CK6, and the positions of the Kozak sequences or splicing units are different from ours [11]. These differences might greatly influence the timing and levels of microdystrophin expression. A second possible factor

doi:10.1016/j.ymthe.2004.07.025

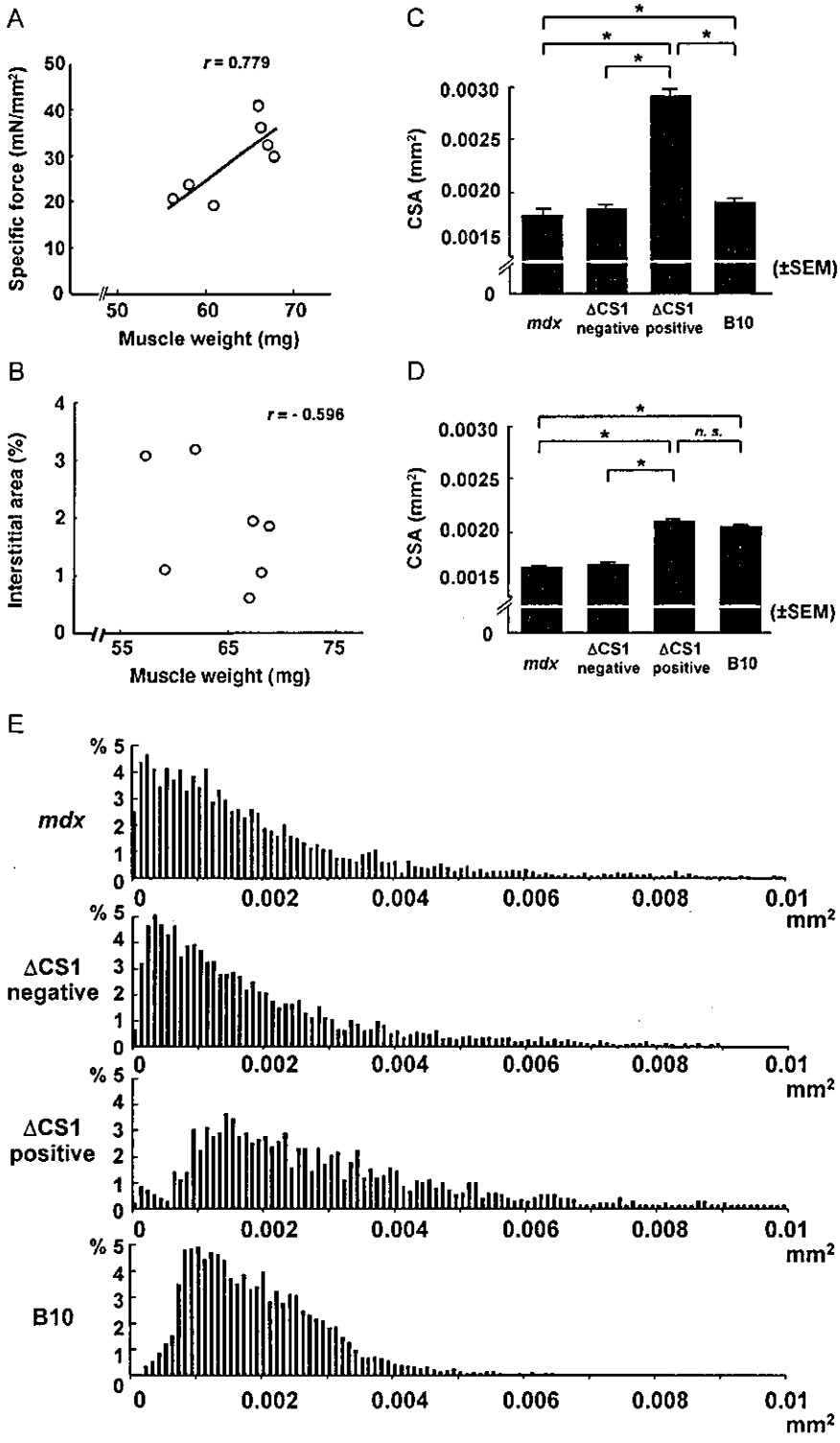

FIG. 4. ΔCS1-positive *mdx* fibers in AAV-treated muscle at 10 days of age show hypertrophy. TA muscles of *mdx* mice were injected with AAV2-MCKΔCS1 at 10 days of age (A–C, E) or at 5 weeks of age (D) and analyzed at 24 weeks after injection. (A) Correlation between muscle wet weight and tetanic force generation ($n = 7$). There was a significant positive correlation between muscle weight and force generation ($r = 0.779$, $P < 0.01$). (B) Relationship between muscle weight and relative interstitial area in AAV-injected muscles ($n = 7$). The increase in muscle weight is not proportional to the interstitial area. (C, D) Mean cross-sectional area (CSA) of uninjected *mdx* muscle fibers and ΔCS1-positive or -negative fibers in AAV-injected *mdx* muscles or age-matched B10 muscle fibers. Three TA muscles were examined for each group. The total numbers of fibers traced were 9674, 6347, 1525, and 5877 in (C) and 8077, 4075, 3479, and 5476 in (D) for *mdx*, ΔCS1-negative *mdx*, ΔCS1-positive *mdx*, and B10 fibers, respectively. When injected at 10 days of age, the CSA of ΔCS1-positive *mdx* fibers was definitely larger than that of normal B10, ΔCS1-negative *mdx*, or contralateral *mdx* fibers (C). In contrast, when mice were treated at 5 weeks of age, the mean CSA of ΔCS1-positive *mdx* fibers was similar to that of B10 muscle and slightly larger than that of *mdx* or ΔCS1-negative *mdx* fibers in treated muscle (D). $^*P < 0.01$. (E) Distribution of the fiber CSAs of untreated *mdx*, ΔCS1-positive, or ΔCS1-negative fibers in *mdx* muscles injected at 10 days of age and age-matched B10 fibers. Shown are the same data set presented in (C). In untreated *mdx* muscles or in ΔCS1-negative *mdx* fibers, small-caliber fibers are dominant, reflecting regeneration. The distribution pattern of ΔCS1-positive fibers deviated to the right, reflecting a larger size than that of B10 fibers. Similar to B10 muscles, small-caliber fibers were markedly reduced in ΔCS1-positive *mdx* fibers, indicating that ΔCS1 prevented muscle degeneration.

is the difference in muscle types used. Harper *et al.* injected AAV vectors into gastrocnemius muscles of 32-day-old mice. The gastrocnemius shows less centrally nucleated fibers than TA muscle in the natural course of the disease (Yuasa *et al.*, unpublished data). In our result, however, AAV-treated *mdx* muscle with a high